AIP | Applied Physics Letters

# Origin of reduction in phonon thermal conductivity of microporous solids

Patrick E. Hopkins, Peter T. Rakich, Roy H. Olsson, Ihab F. El-kady, and Leslie M. Phinney

Citation: Appl. Phys. Lett. **95**, 161902 (2009); doi: 10.1063/1.3250166
View online: http://dx.doi.org/10.1063/1.3250166
View Table of Contents: http://apl.aip.org/resource/1/APPLAB/v95/i16
Published by the American Institute of Physics.

## Related Articles

Enhanced phonon scattering by mass and strain field fluctuations in Nb substituted FeVSb half-Heusler thermoelectric materials
J. Appl. Phys. 112, 124915 (2012)

Ab initio simulation of hydrogen bonding in ices under ultra-high pressure
J. Chem. Phys. 137, 204507 (2012)

Plasmon-induced fluorescence and electroluminescence from porphine molecules on GaAs(110) in a scanning tunneling microscope
Appl. Phys. Lett. 101, 203107 (2012)

Imaging of a patterned and buried molecular layer by coherent acoustic phonon spectroscopy
Appl. Phys. Lett. 101, 191606 (2012)

Influence of crystallographic orientation and anisotropy on Kapitza conductance via classical molecular dynamics simulations
J. Appl. Phys. 112, 093515 (2012)

## Additional information on Appl. Phys. Lett.

Journal Homepage: http://apl.aip.org/
Journal Information: http://apl.aip.org/about/about_the_journal
Top downloads: http://apl.aip.org/features/most_downloaded
Information for Authors: http://apl.aip.org/authors

ADVERTISEMENT

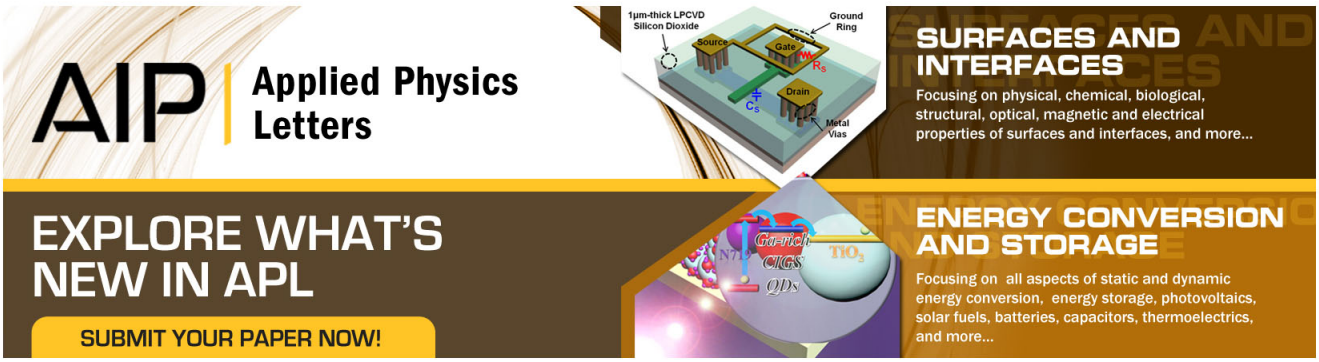

# Origin of reduction in phonon thermal conductivity of microporous solids

Patrick E. Hopkins,[a] Peter T. Rakich, Roy H. Olsson, Ihab F. El-kady, and Leslie M. Phinney
*Sandia National Laboratories, Albuquerque, New Mexico 87185-0346, USA*

(Received 7 July 2009; accepted 25 September 2009; published online 20 October 2009)

Porous structures have strong tunable size effects due to increased surface area. Size effects on phonon thermal conductivity have been observed in porous materials with periodic voids on the order of microns. This letter explores the origin of this size effect on phonon thermal conductivity observed in periodic microporous membranes. Pore-edge boundary scattering of low frequency phonons explains the temperature trends in the thermal conductivity; further reduction in thermal conductivity is explained by the porosity. © *2009 American Institute of Physics*.
[doi:10.1063/1.3250166]

Size effects significantly impact phonon thermal transport in micro- and nanoscale systems.[1] Thorough understanding of such effects is crucial to the study of thermal transport in micro- and nanosystems and for continued advancement of novel applications, such as thermoelectrics.[2–5] In particular, porous structures are known to have strong tunable size effects due to increased surface area.[6,7] While electron thermal size effects have been observed on nanometer length scales in porous structures,[8] phonon thermal size effects have been observed on micron length scales.[9] This has substantial impact on phononic crystal structures, which provide novel material solutions for thermoelectric applications.[10] In this letter, we explain the origin of phonon size effects on thermal conductivity reduction in periodic microporous silicon membranes. We begin by constructing a model for the thermal conductivity of microporous materials based on phonon thermal transport and compare this model to recent experimental findings by Song and Chen.[9] These data were earlier compared with models accounting for the membrane porosity but not the spectral nature of the phonon thermal transport.[9] The spectral contribution of the various phonon modes is presented which shows that the origin of the temperature dependency of the thermal conductivity reduction is attributed to low frequency phonon boundary scattering off the porous media boundaries.

To model the effects of porosity on the thermal conductivity, we use a procedure similar to that outlined by Holland[11] to capture the effects of scattering on certain phonon frequencies and modes. Through this model, the thermal conductivity is given by

$$\kappa = \frac{1}{6\pi}\sum_j \int_q \frac{\hbar^2\omega_j^2(q)}{k_B T^2} \frac{\exp\left[\frac{\hbar\omega_j(q)}{k_B T}\right]}{\left(\exp\left[\frac{\hbar\omega_j(q)}{k_B T}\right]-1\right)^2} v_j^2(q)\tau_j(q)q^2 dq, \tag{1}$$

where $\hbar$ is the reduced Planck's constant, $\omega(q)$ is the phonon dispersion, $k_B$ is the Boltzmann constant, $T$ is the phonon temperature, $v(q)=\partial\omega(q)/\partial q$ is the phonon group velocity, $\tau(q)$ is the scattering time of the phonons, $q$ is the wave vector, and the thermal conductivity, $\kappa$, is summed over $j=3$ modes (one longitudinal and two transverse). To evaluate this expression, we must determine the Si dispersion and scattering times. We use measured bulk Si dispersion data in the [1,0,0] direction[12,13] and fit the data to a fourth degree polynomial for an analytical expression for $\omega(q)$ and $v(q)=\partial\omega(q)/\partial q$.[14] In bulk Si, phonon scattering is dominated by Umklapp, impurity, and boundary scattering, which are given by[15] $\tau_{\text{Umklapp},j}^{-1}=BT\omega_j^2(q)\exp[C/T]$, $\tau_{\text{impurity},j}^{-1}=D\omega_j^4(q)$, and $\tau_{\text{boundary},j}^{-1}=v_j(q)/E$, respectively, where $B$, $C$, $D$, and $E$ are constants determined by fitting Eq. (1) to data. These scattering times are related to the total phonon scattering time in Eq. (1) via Mattheissen's Rule,

$$\frac{1}{\tau_j(q)} = \frac{1}{\tau_{\text{Umklapp},j}} + \frac{1}{\tau_{\text{impurity},j}} + \frac{1}{\tau_{\text{boundary},j}}. \tag{2}$$

Using Eq. (2) to evaluate Eq. (1), the thermal conductivity of Si is calculated and the coefficients in the various scattering times are iterated to achieve a best fit with measured data on bulk Si.[16] Figure 1 shows the model fit to the data. The inset of Fig. 1 shows the measured dispersion of Si and the poly-

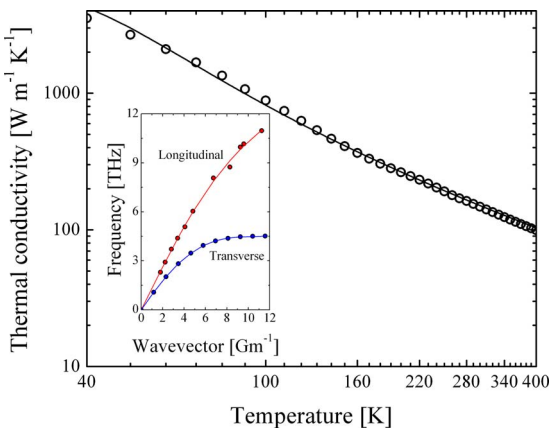


FIG. 1. (Color online) Thermal conductivity model fit to experimental data on single crystalline Si (Ref. 16). The best fit coefficients for the various scattering times are $B=3.73\times10^{-19}$ s K$^{-1}$, $C=157.3$ K, $D=9.32\times10^{-45}$ s$^3$, and $E=2.3\times10^{-3}$ m. (Inset) Dispersion data from bulk Si (Refs. 12 and 13) and polynomial fit. The fourth order polynomial fit has the form $\omega(q)=A_4q^4+A_3q^3+A_2q^2+A_1q$. For the longitudinal branch, the coefficients $A_4$, $A_3$, $A_2$, and $A_1$, are $1.37\times10^{-27}$ m$^4$ s$^{-1}$, $-3.53\times10^{-17}$ m$^3$ s$^{-1}$, $2.94\times10^{-8}$ m$^2$ s$^{-1}$, and 8350 m s$^{-1}$, respectively. For the transverse branch, the coefficients are $1.94\times10^{-27}$ m$^4$ s$^{-1}$, $-3.36\times10^{-17}$ m$^3$ s$^{-1}$, $1.86\times10^{-7}$ m$^2$ s$^{-1}$, and 6090 m s$^{-1}$, respectively.

[a]Author to whom correspondence should be addressed. Tel.: 505.284.5729. Electronic mail: pehopki@sandia.gov.

 

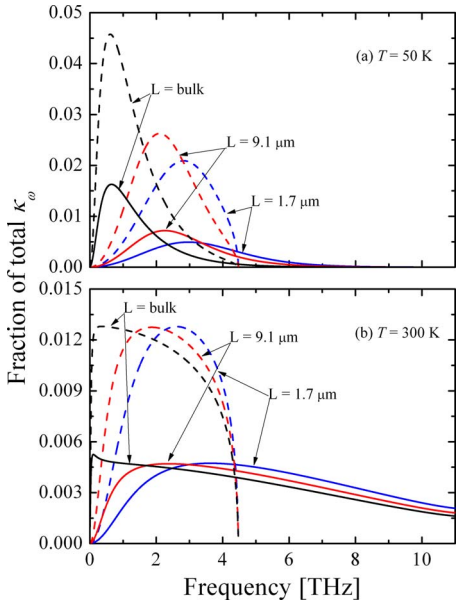


FIG. 2. (Color online) Fraction of the total spectral thermal conductivity at (a) 50 and (b) 300 K for $L=\infty$ (no void boundaries), 9.1, and 1.7 $\mu$m, where $L$ is the distance between void boundaries. The longitudinal components are shown by the solid lines and the transverse components by the dashed lines.

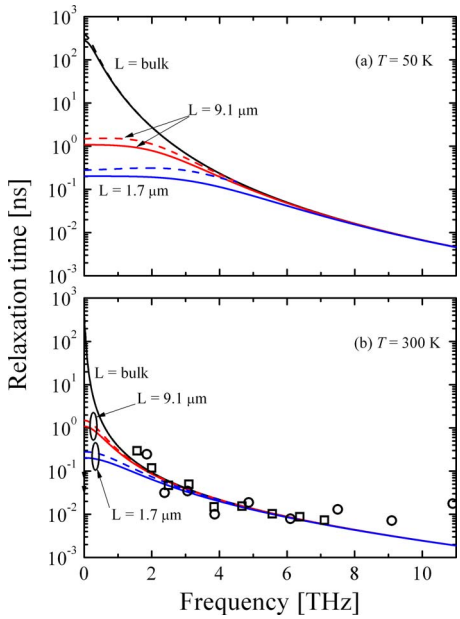


FIG. 3. (Color online) Relaxation time of the longitudinal (solid lines) and transverse (dashed lines) as a function of frequency for (a) $T=50$ K and (b) $T=300$ K. For comparison, relaxation times calculated with MD simulations for bulk Si at 300 K are shown (Ref. 21). The circles represent the longitudinal modes and the squares the transverse modes.

nomial fit. We assume the transverse branch is doubly degenerate. The boundary scattering determined from the fit in Fig. 1 does not represent internal boundaries, such as grain boundaries or nanomaterial boundaries,[8,17–19] since Eq. (4) is used to fit Eq. (1) to bulk, single crystalline Si data.

With all the parameters determined for the case of solid single crystalline Si, $\kappa_{\text{solid}}$, the effects of periodic voids in the crystal are considered. The first aspect of the phonon transport that must be considered is scattering off the edges of the voids in the porous structure. To model this, we treat the scattering process as scattering from phonons at grain boundaries given by[18] $\tau^{-1}_{\text{internal},j}=v_j(q)/L$, where $L$ is the distance between void boundaries. We consider two distances to match the Si microporous membranes that have been previously experimentally studied,[9] $L=9.1$ and 1.7 $\mu$m. We estimate the dominant thermal wavelength of Si at 40 K as 1.25 nm assuming $\lambda_{\text{thermal}}\approx hv_{\text{av}}/(k_BT)$ where $v$ is the average phonon velocity, which we take as 6545 m s$^{-1}$.[20] The scale of the dominant thermal wavelength serves as strong justification of our use of a bulk dispersion relation of Si since the distance between the periodic voids that we consider in this paper are nearly three orders of magnitude greater than the thermal wavelength.

To understand how the thermal conductivity of the Si crystal will be impacted by boundary scattering at these distances, we analyze the spectral contribution to thermal conductivity, which is given by

$$\kappa_{\omega,j}=\frac{1}{6\pi}\frac{\hbar^2\omega_j^2(q)}{k_BT^2}\frac{\exp\left[\frac{\hbar\omega_j(q)}{k_BT}\right]}{\left(\exp\left[\frac{\hbar\omega_j(q)}{k_BT}\right]-1\right)^2}v_j(q)\tau_j(q)q^2. \quad (3)$$

Here the transverse spectral thermal conductivity is multiplied by 2 since we assume doubly degenerate transverse branches. Figure 2 shows the fraction of the total spectral thermal conductivity at (a) 50 and (b) 300 K for $L=\infty$ (no void boundaries), 9.1, and 1.7 $\mu$m. This fraction is defined as $\kappa_{\omega,j}/\Sigma_j\Sigma_\omega\kappa_{\omega,j}$. As the scattering distance decreases, the dominant phonon frequencies participating in transport increase. This implies that the low frequency (long wavelength) phonons are being scattered or "impeded" most drastically, explaining the significant thermal conductivity reduction with decreasing temperature. At low temperatures, [Fig. 2(a), $T=50$ K], the dominant phonon frequencies responsible for heat transport are relatively low. Thus, introducing periodic boundaries (producing features of micron dimensions) has significant impact on the phonons participating in transport. As temperatures increase [Fig. 2(b), $T=300$ K], the dominant phonon frequencies increase; however, scattering of the low frequency phonons (most strongly impacted by the microporous structure) does not affect the thermal conductivity as drastically.

To understand this in more detail, Fig. 3 shows the relaxation time as a function of frequency for the cases considered in Fig. 2. The relaxation time decreases as the boundary length decreases, but the relaxation times of all three cases converge at higher frequencies [recall that the relaxation time is directly related to the mean free path through Matthiessen's Rule, seen in Eq. (2)]. From Matthiessen's rule, we see that the relaxation times of the lower frequency phonons, having larger intrinsic mean free paths, are affected more drastically by scattering from pore boundaries than the higher frequency phonons, which have smaller mean free paths. Since the relaxation times of the low frequency phonons are severely reduced, the spectral contribution of thermal conductivity is dominated by higher frequency phonons as the boundary scattering distance decreases (as predicted by Fig. 2). Also, as temperature decreases, the relaxation time does not decrease as rapidly as a function of frequency, leading to a larger mean free path of phonons at higher frequencies. This causes scattering of higher frequency phonons at lower temperatures leading to a further decrease in thermal conductivity. We have included the fre-

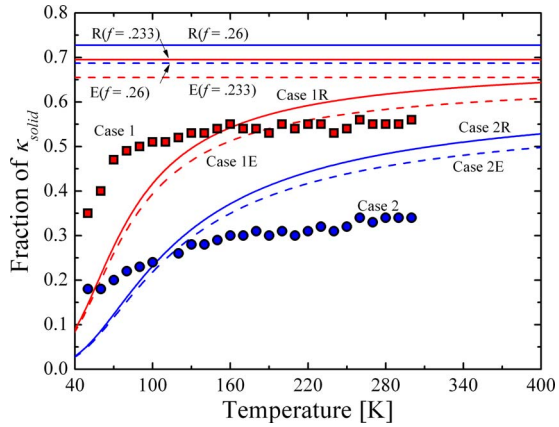


FIG. 4. (Color online) Calculated thermal conductivity accounting for pore boundary scattering for two porous Si structures studied by Song and Chen. The $L=9.1$ $\mu$m (case 1) structure has a porosity of 23.3% and the $L=1.7$ $\mu$m (case 2) structure has a porosity of 26%. The data collected by Song and Chen are also shown in this figure along with the reduction in thermal conductivity predicted by the $R$ (solid lines) and $E$ (dashed lines) models without assuming boundary scattering. The scattering of phonons off the pore boundaries explains the temperature trend in the reduction in thermal conductivity of the two microporous Si structures. The porosity alone explains some of the reduction, but does not capture the full reduction nor the temperature trend in the thermal conductivity reduction.

quency dependent relaxation time calculated on bulk Si using molecular dynamics (MD) simulations by Henry and Chen[21] for comparison. The MD simulations agree well with our calculated values and trends of bulk Si relaxation time. The deviation at high frequencies in the longitudinal modes does not affect our thermal conductivity calculations since high frequency longitudinal modes do not significantly contribute to thermal conductivity at room temperature, as seen in Fig. 2(b). Furthermore, we calculate the contribution of longitudinal phonons above 9.0 THz to contribute less than 4% to the overall thermal conductivity.

Further reductions in $\kappa_{solid}$ must be accounted for by the porous nature of the structure, as less silicon is present in the porous structure that in its unpatterned counterpart. To account for this reduction in material, we choose two simplified models based on Fourier heat conduction theory. The $R$ model, derived by Russell,[22] is given by $\kappa_{porous}/\kappa_{solid}=(1-\phi^{2/3})/(1-\phi^{2/3}+\phi)$, where $\phi$ is the porosity. The $E$ model, derived by Eucken,[23] is given by $\kappa_{porous}/\kappa_{solid}=(1-\phi)/(1+\phi/2)$. Figure 4 shows the calculated thermal conductivity accounting for pore boundary scattering for two porous Si structures studied by Song and Chen.[9] The $L=9.1$ $\mu$m (Case 1) structure has a porosity of 23.3% and the $L=1.7$ $\mu$m (Case 2) structure has a porosity of 26%. The data collected by Song and Chen are also shown in this figure along with the reduction in thermal conductivity predicted by the $R$ and $E$ models without assuming boundary scattering. The scattering of phonons off the pore boundaries explains the temperature trend in the reduction in thermal conductivity of the two microporous Si structures. The porosity alone explains some of the reduction, but does not capture the full reduction or the temperature trend in the thermal conductivity reduction.

In conclusion, this letter has theoretically examined the origin of the phonon thermal conductivity reduction in microporous solids using an analytical expression for the bulk phonon dispersion in Si. By analyzing the spectral contribution to thermal conductivity and the dependence on relaxation time with phonon frequency, the majority of the reduction in thermal conductivity of porous materials is associated with low frequency phonon scattering off the pore boundaries, which also explains the temperature trends in $\kappa_{porous}/\kappa_{solid}$ observed in recent data on porous Si structures. Further reduction in thermal conductivity is ascribed to the porous nature of the solid.

P.E.H. acknowledges funding by the Harry S. Truman Fellowship through the LDRD Program at Sandia National Laboratories. The authors thank Edward S. Piekos for insightful discussions. Sandia is a multiprogram laboratory operated by Sandia Corporation, a Lockheed-Martin Co. for the United States Department of Energy's National Nuclear Security Administration under Contract No. DE-AC04-94Al85000.

[1] D. G. Cahill, W. K. Ford, K. E. Goodson, G. D. Mahan, A. Majumdar, H. J. Maris, R. Merlin, and S. R. Phillpot, J. Appl. Phys. **93**, 793 (2003).
[2] A. I. Boukai, Y. Bunimovich, J. Tahir-Kheli, J.-K. Yu, W. A. Goddard, and J. R. Heath, Nature (London) **451**, 168 (2008).
[3] G. Chen, ASME J. Heat Transfer **119**, 220 (1997).
[4] M. S. Dresselhaus, G. Dresselhaus, X. Sun, Z. Zhang, S. B. Cronin, T. Koga, J. Y. Ying, and G. Chen, Microscale Thermophys. Eng. **3**, 89 (1999).
[5] S. Riffat and X. Ma, Appl. Therm. Eng. **23**, 913 (2003).
[6] G. Benedetto, L. Boarino, and R. Spagnolo, Appl. Phys. A: Mater. Sci. Process. **64**, 155 (1997).
[7] U. Bernini, R. Bernini, P. Maddalena, E. Massera, and P. Rucco, Appl. Phys. A: Mater. Sci. Process. **81**, 399 (2005).
[8] P. E. Hopkins, P. M. Norris, L. M. Phinney, S. A. Polycastro, and R. G. Kelly, J. Nanomater. **2008**, 418050 (2008).
[9] D. Song and G. Chen, Appl. Phys. Lett. **84**, 687 (2004).
[10] R. H. Olsson III and I. El-Kady, Meas. Sci. Technol. **20**, 012002 (2009).
[11] M. G. Holland, Phys. Rev. **132**, 2461 (1963).
[12] G. Nilsson and G. Nelin, Phys. Rev. B **6**, 3777 (1972).
[13] B. N. Brockhouse, Phys. Rev. Lett. **2**, 256 (1959).
[14] E.S. Piekos, S. Graham, and C.C. Wong, Sandia National Laboratories Report No. SAND2004-0531, 2004.
[15] G. Chen, *Nanoscale Energy Transport and Conversion: A Parallel Treatment of Electrons, Molecules, Phonons, and Photons* (Oxford University Press, New York, 2005).
[16] C. Y. Ho, R. W. Powell, and P. E. Liley, J. Phys. Chem. Ref. Data **1**, 279 (1972).
[17] A. D. McConnell and K. E. Goodson, Annu. Rev. Heat Transfer **14**, 129 (2005).
[18] A. D. McConnell, S. Uma, and K. E. Goodson, J. Microelectromech. Syst. **10**, 360 (2001).
[19] P. E. Hopkins, J. Appl. Phys. **105**, 093517 (2009).
[20] D. E. Gray, *American Institute of Physics Handbook*, 3rd ed. (McGraw-Hill, New York, 1972).
[21] A. S. Henry and G. Chen, J. Comput. Theor. Nanosci. **5**, 1 (2008).
[22] H. W. Russell, J. Am. Ceram. Soc. **18**, 1 (1935).
[23] A. Eucken, Forschung auf dem Gebiete des Ingenieurwesens, Ausgabe B, Band 3, 3/4 VDI Forschungsheft 353 (1932).